Chapter1

Introduction

Chromium is a chemical element symbolized by Cr with atomic number 24. The electronic configuration is $[Ar]3d^5 4s^1$. The highest oxidation state is that corresponding to the total number of 3d and 4s electrons. The oxidation states are -II, -I, 0, I, II, III, IV, V, and VI. The most stable and important state is Cr^{III}, d^3, which in an octahedral complex has each t_{2g} level singly occupied, giving a sort of half-filled shell stability (Cotton and Wilkinson, 1972). Chromium (III) has a strong tendency to bind oxygen containing functional groups and form complexes with organic ligands, including oxalate, citrate, malonate, EDTA, and DTPA, which are soluble and stable within environmental pH range. (Mytych et al., 2005)

Aluminium is a chemical element symbolized by Al with atomic number 13. The element is a hard, strong, and white metal. Elemental aluminium itself is clearly metallic and ionic in their character. It is the group IIIA element in the Periodic Table. The electronic configuration is $[Ne]3s^2 3p^1$ as a result the trivalent state is its most important state. It is the commonest metallic element in the earth's crust and occurs widely in nature in silicates such as micas and feldspares (Cotton and Wilkinson, 1972).

The oxalate ion is a versatile ligand since it can act as a mono-, bi-, tri-, and tetradentate ligand (Figure 1) capable of forming bridged polynuclear complexes. Much interesting exists in the oxalate ligand as a bridging unit for preparing polynuclear complexes and extended molecular assemblies in order to study magnetic ordering behavior. From a structural point of view, ionic, chain, and layer structures are known. With tripositive transition metal ions, the tris chelate anions $[M^{III}(C_2O_4)_3]^{3-}$ are formed. (Decurtins et al., 1993)

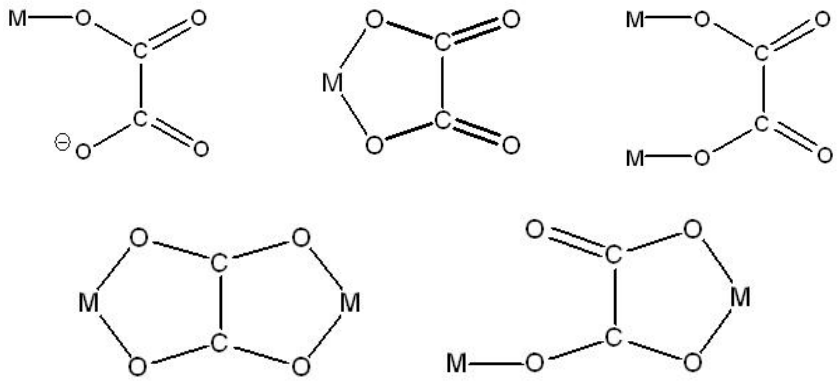

Figure 1 Oxalato complexes (Cotton and Wilkinson, 1988)

Moreover, oxalate can act as a bridging unit for polynuclear complexes and extended molecular assemblies, not only owing to their potential magnetostructural properties but also due to the fact that polynuclear oxalate system are excellent candidates to improve our still very limited understanding of the way that molecules and ions are organised in the solid state to form materials with given physical and chemical properties.(Román et al., 1996)

Generally, alkali oxalate play an important role in nature and chemistry. The sodium and potassium salts of oxalic acid are found in many plants (clover, sorrel, salicornia, spinach, rhubarb, bambo shoots, cacao, roots, and tree barks). Oxalates find some technical and medical applications such as stain removal in photography, metal coatings for stainless steel, nickel, chromium, titanium, and their alloys, cleaning and bleaching of natural fibers, textile dyeing, anticoagulants in medical tests, and dental seals. Furthermore potassium and sodium oxalate complexes are able to pass the gastric mucous membrane, and therefore they are the main components of kidney stones (Dinnebier et al., 2003) .

In addition, the salts based on oxalate complexes are interesting materials, which have technological applications as precursors to nanocrystalline metallic oxides

(Delgado et al., 2002) such as the work by Youssef (1986) that reported thermal decomposition on of some oxalates, being precursor of oxide.

Especially, the tris-chelated $[M(C_2O_4)_3]^{3-}$ complex (M=trivalent first row transition) is well known ligand in the preparation of heterometallic complexes when using the so-called building block strategy. It has been found that its reaction with transition metal ions can lead to infinite two- and three-dimensional magnetic networks depending on the nature of the templating cation (Armentano et al., 2001) .

The crystal structures of trioxalate metallate salts of general formula $M^{I}_3M^{III}(C_2O_4)_3 \cdot 3H_2O$, with M^{I}=K, Rb, NH_4 and M^{III}=Al, Cr, Ga, Fe, Mn have been reported as monoclinic cells, space group $P2_1/c$, or as triclinic cells, space group $P\bar{1}$. The structures consist of $[M^{III}(C_2O_4)_3]^{3-}$ moieties, with M^{III} atoms coordinated octahedrally to three oxalate groups acting as bidentate ligands (Delgado et al., 2002).

In the recent work, many papers reported their interests on $[Cr(C_2O_4)_3]^{3-}$ doped in the crystalline hosts, for examples, the exitation energy transfer properties of $[Cr(C_2O_4)_3]^{3-}$ chromophores in $[Rh(bpy)_3][NaAl_{1-x}Cr_x(C_2O_4)_3]ClO_4$ (von Arx et al., 2002), the effect of changing environment on the $^2E \rightarrow {}^4A_2$ emission of $[Cr(C_2O_4)_3]^{3-}$ in 13 crystal lattices (Coleman, 1975), the spin Hamiltonians of $[Cr(C_2O_4)_3]^{3-}$ in $K_3Al(C_2O_4)_3 \cdot 3H_2O$ (Doetschman, 1974), $(NH_4)_3Al(C_2O_4)_3 \cdot 2H_2O$, $Na_3Al(C_2O_4)_3 \cdot 5H_2O$ (Kawasaki et al., 1969), $NaMgAl(C_2O_4)_3 \cdot 9H_2O$ (Bernheim and Reichenbecher, 1969). These compounds are interesting because of their optical properties. The Cr^{3+} doped complexes were shown to be promising materials for tunable laser applications in the near IR region.

In the work by Laongjit (M.S.Thesis, 2004), oxalato complexes of chromium and aluminium with oxalate as bridging ligand were synthezied and characterized. The chemical properties of the complexes were studied by X-ray diffraction and spectroscopic techniques such as single crystal X-ray, FT-IR, UV-Vis, SEM/EDX, ICP-AES, TGA, and DSC techniques.

In this present work, oxalato complexes of chromium and aluminium were further characterized by UV-Vis, ^{13}C-NMR, and EPMA/EDX. The products were prepared by the same method but with the amount of $K_3[Cr(C_2O_4)_3]\cdot 3H_2O$ varied and were characterized by ICP-AES and WDXRF.

1.2 Literature reviews

Kawasaki (1969) synthesized $[Cr(C_2O_4)_3]^{3-}$ complex in the crystalline hosts $K_3Al(C_2O_4)_3\cdot 3H_2O$, $(NH_4)_3Al(C_2O_4)_3\cdot 2H_2O$, and $Na_3Al(C_2O_4)_3\cdot 5H_2O$ and observed by ESR spectroscopy then compared with the Cr^{3+}: $NaMgAl(C_2O_4)_3\cdot 9H_2O$ results. He found that the D^* parameter (0.72 ± 0.06 cm^{-1}) is relatively insensitive to environment but E^* varies from zero to 0.1 cm^{-1} (D^* and E^* are the spin Hamiltonian parameter).

Doetschman (1974) synthesized $[Cr(C_2O_4)_3]^{3-}$ complex in single $K_3Al(C_2O_4)_3\cdot 3H_2O$ crystals and studied by EPR. The complexes and their environments were asymmetric. The crystals were grown at room temperature from a saturated aqueous solution of 0.005g $K_3Cr(C_2O_4)_3\cdot 3H_2O$ and 0.335g $K_3Al(C_2O_4)_3\cdot 3H_2O$ by slowly evaporating the solvent by passing N_2 through the flask containing the solution. The small blue crystals grew at temperature as low as 80 K due to the loss of water.

Taylor (1978) reported crystal structure of the isomorphous complexes $K_3M(C_2O_4)_3\cdot 3H_2O$, M=$Cr^{III}$ and Al^{III} with the data as shown below.

General formula	system	a (Å)	b (Å)	c (Å)	β (°)
$K_3Al(C_2O_4)_3\cdot 3H_2O$	monoclinic	7.712	19.518	10.286	108.21
$K_3Cr(C_2O_4)_3\cdot 3H_2O$	monoclinic	7.714	19.687	10.361	108.26

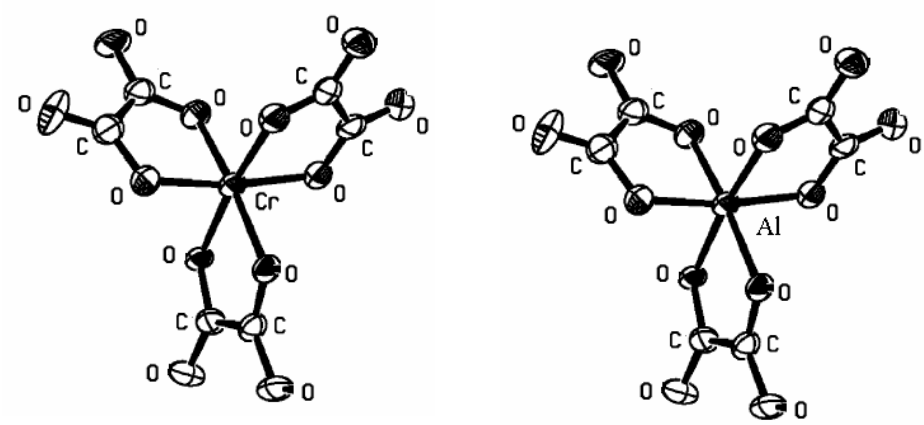

Figure 2 A stereoview of the $[Cr(C_2O_4)_3^{3-}]$ anion and $[Al(C_2O_4)_3^{3-}]$ anion (Taylor, 1978)

Yager et al., (1979) studied both spin allowed and spin forbidden electronic transition in $[Cr(C_2O_4)_3]^{3-}$. Visible spectroscopy of 10^{-2}M $K_3Cr(C_2O_4)_3$ yielded spectra with convenient absorbance for the allowed bands and a clearly visible forbidden to be observed (Table 1).

Table 1 Assignment of transitions in the $[Cr(C_2O_4)_3]^{3-}$ spectrum

Band maximum		ε(M^{-1} cm^{-1})	Assignment
nm	cm^{-1}		
420	23,800	98	$^4A_2 \rightarrow {}^4T_1$
570	17,500	76	$^4A_2 \rightarrow {}^4T_2$
698	14,300	3	$^4A_2 \rightarrow {}^2E, {}^2T_1$

Schönherr et al., (1989) synthesized Cr^{3+} doped in $NaMgAl(C_2O_4)_3 \cdot 8H_2O$ and reported results on single-crystal emission and polarized absorption spectra. Since the chromium occupied equivalent position the band pattern arising from spin-forbidden transitions was less complicated compared to the corresponding compound of nine-crystalline water. Anisotropic electric dipole selection rules allowed for assignments of the Kramers doublets resulting from ^2E_g(Oh) which is split by only 2-3 cm^{-1}.

Román et al., (1996) synthsized $[Ni(bipy)_3][NaAl(C_2O_4)_3]$ by mixing of $K_2[Ni(C_2O_4)_2(H_2O)_2]\cdot 4H_2O$ and $[H_2bipy]Cl_2$ in silica hydrogel at room temperature. The complex, which incorporates Na and Al from the silica gel, was characterized by IR, energy-dispersive X-ray analysis, thermogravimetric techniques and single-crystal X-ray diffraction. It crystallized in the cubic system, space group $P2_13$, with a= 15.518Å. The crystal structure consisted of a chiral, three-dimensional polymeric network of Al^{3+} and Na^{+} bridged by bis(bidentate oxalate) ligands, $[NaAl(C_2O_4)_3]_n^{2n-}$, with the $[Ni(bipy)_3]^{2+}$ cation inserted in the anionic network cavities. The cationic and anionic networks were held together by means of electrostatic forces and weak C-H ···O hydrogen bonds.

Dardene (1999) explained the relationship between color and chemical composition in a series of Mn(V)-substituted fluoroapatites $A_{10}(B_{1-x}Mn_xO_4)_6F_2$; A=Ca, Sr, Ba; B=P, V, with the Mn substitution = x. These apatites exhibited deep blue to green colors. Saturation effects occured for some tetrahedral Mn(V) absorption bands, which were correlated to the large cross section of the corresponding transitions. These accounted for the blue to green color change with increasing the Mn content, x. The crystal field experienced by the Mn(V) ion was independent of x and of the nature of the B ion it replaced. This was because Mn(V) imposed its own size to the host lattice (mean Mn-O distance 51.72 Å in all cases). The displacement of the Mn(V) absorption bands for A over the series Ca, Sr, to Ba was mainly due to an increasing Mn-O bond covalency.

Langford et al., (1999) synthesized two series of mixed crystals of nominal compositions $[NaAl_{1-x}Cr_x(C_2O_4)_3][Rh_{0.99}Cr_{0.01}(bpy)_3]ClO_4$ (x = 0, 0.01, 0.05, 0.1, 0.2, 0.4, 0.6, 0.8, and 1) and $[NaAl_{0.99}Cr_{0.01}(C_2O_4)_3][Rh_{1-y}Cr_y(bpy)_3]ClO_4$ (y = 0, 0.01, 0.02, 0.03, 0.04, and 0.05) and studied about electronic energy transfer from $[Cr(C_2O_4)_3]^{3-}$ in three-dimensional anionic oxalate network to encapsulated $[Cr(bpy)_3]^{3+}$ cation by time-resolved luminescence spectroscopy. Energy transfer from $[Cr(C_2O_4)_3]^{3-}$ to$[Cr(bpy)_3]^{3+}$

occured by two mechanisms. Rapid, short-range transfer ($k_{et} > 10^6$ s^{-1}) is attributed to superexchange coupling between the Cr^{3+} ions through π overlap of the oxalate and bipyridine ligands.

Hermanowicz (2001) studied $KCr_xAl_{1-x}(MoO_4)_2$ and $NaCr_xAl_{1-x}(MoO_4)_2$ crystals (x varies from 0% to 2%) at temperatures ranging from 15 to 300 K by infrared, Raman, absorption, excitation and emission spectra as well as electron spin resonance. A very rich vibronic structure of the emission band was explained and assigned to the respective vibrational modes. One Cr^{3+} center characterized by 2.1 and 2.8 ms lifetimes (at 15 K) for the sodium and potassium derivative, respectively, for the $^2E \rightarrow {}^4A_2$ transition was identified for both the crystals. The phase transition from trigonal to monoclinic space group was discovered at about 60K for $KAl(MoO_4)_2 : Cr^{3+}$ crystal. Cr^{3+} doped molybdates were shown to be promising materials for tunable laser applications in the 1 μm wavelength region. The Cr^{3+} doped trigonal $KAl(MoO_4)_2$ and monoclinic $NaAl(MoO_4)_2$ were new materials with very promising optical properties. The single crystals could be grown easily from the melt with high doping levels and without any traces of color centers.

Martin et al., (2001) synthesized $(BEDT\text{-}TTF)_4[A^IM^{III}(C_2O_4)_3]\cdot PhCN$, where $A^I = H_3O$, NH_4, K; M^{III} = Cr, Fe, Co, Al; BEDT-TTF = bis(ethylenedithio)tetrathiafulvalene. They reported structure by single-crystal X-ray diffraction, and physical properties. In the monoclinic series each layer contained one enantiomeric conformation of the chiral $[M(C_2O_4)_3]^{3-}$ anions with alternate layers having opposite chirality, whereas in the orthorhombic series the enantiomers formed chains within each layer. Analysis of the supramolecular organization at the interface between the cation and anion layers showed that this difference was responsible for the two different BEDT-TTF packing motifs, as a consequence of weak H-bonding interactions between the terminal ethylene groups in the donor and the $[M(C_2O_4)_3]^{3-}$ oxygen atoms.

Table 2 Summary of Crystal data for selected compounds with the stoichiometry $(BEDT\text{-}TTF)_4[A^IM^{III}(C_2O_4)_3]\cdot PhCN$ (Martin et al., 2001)

	I	**II**	**III**	**IV**	**V**	**VI**
M^{III}	Co	Al	Fe	Cr	Cr	Fe
A^I	NH_4	NH_4	H_3O	H_3O	H_3O	NH_4
chem formula	$C_{53}H_{41}O_{12}S_{32}CoN_2$	$C_{53}H_{41}O_{12}S_{32}AlN_2$	$C_{53}H_{39}FeN_2O_{13}S_{32}$	$C_{53}H_{37}O_{13}S_{32}CrN$	$C_{53}H_{39}O_{13}S_{32}CrN$	$C_{53}H_{41}FeN_2O_{12}S_{32}$
a/Å	10.340(10)	10.318(7)	10.232(12)	10.240(1)	10.371(2)	10.370(5)
b/Å	19.5016(2)	19.460(4)	20.04(3)	19.965(1)	19.518(3)	19.588(12)
c/Å	35.7684(5)	35.808(8)	34.97(2)	34.905(1)	35.646(2)	35.790(8)
β/deg	90.0	90.0	93.25(11)	93.69(1)	90.0	90.0
V/Å	7212.6(14)	7190(5)	7157(13)	7121.6(2)	7216(2)	7270(6)
Z	4	4	4	4	4	4
fw	1982.90	1950.96	1979.78	1973.76	1975.99	1974.61
crys syst	orthorhombic	orthorhombic	monoclinic	monoclinic	orthorhombic	orthorhombic
space group	*Pbcn*	*Pbcn*	*C2/c*	*C2/c*	*Pbcn*	*Pbcn*
T/K	150(2)	150(2)	120(2)	120(2)	150(2)	120(2)

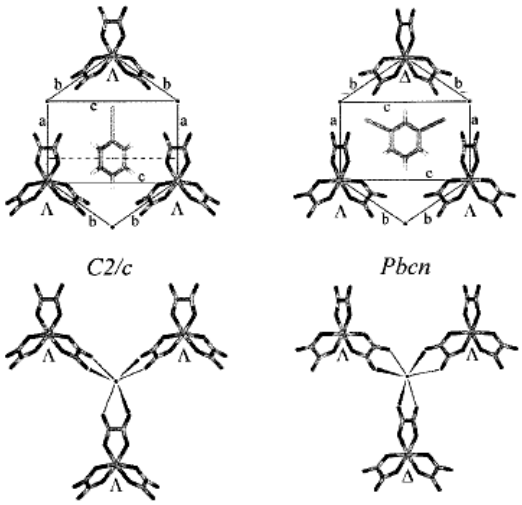

Figure 3 The anionic layer in $(BEDT\text{-}TTF)_4[AM(C_2O_4)_3]\cdot PhCN$ for the monoclinic *C*2/*c* (left) and orthorhombic *Pbcn* (right) structures. (Martin et al., 2001)

Von Arx et al.,(2002) studied resonant energy transfer in the mixed crystal series $[Rh(bpy)_3][NaAl_xCr_{1-x}(C_2O_4)_3]ClO_4]$ (x=0.05-0.9). Efficient resonant energy transfer occured within the R_1 line of the $^4A_2 \rightarrow {}^2E$ transition of $[Cr(C_2O_4)_3]^{3-}$

chromophore in mixed crystal. The result showed that the number of lines and their relative intensities depended critically upon the $[Cr(C_2O_4)_3]^{3-}$concentration and the excitation wavelength within the inhomogeneous distribution.

Bodor et al., 2003 reported identification of $Al(C_2O_4)_{1-3}$ species in 0.6 M aqueous NaCl with ^{13}C-NMR spectroscopy. Rate constants and activation parameters for intramolecular cis/trans isomerisation of Werner-type $[Al(C_2O_4)_2]^-$ complex and a very slow intermolecular ligand exchange reaction of $[Al(C_2O_4)_3]^{3-}$complex and the free ligand were determined by dynamic 1D and 2D ^{13}C-NMR measurment. Mixed complexes, $[AlF(C_2O_4)]$, $[AlF(C_2O_4)_2]^{2-}$, $[AlF_2(C_2O_4)]^-$, and $[AlF_2(C_2O_4)_2]^{3-}$ were measured by potentiometry and confirmed by ^{13}C and ^{19}F-NMR.

Laongjit (M.S.Thesis, 2004) synthesized and characterized oxalato complexes prepared by mixing aqueous solutions of $K_3[Cr(C_2O_4)_3].3H_2O$, $K_3[Al(C_2O_4)_3].3H_2O$ and NaCl at room temperature. Three types of crystals were obtained, two were dark red almost black and the other was blue. They are designated as RedCubic, RedHexagonal, and Blue and characterized by X-ray, FT-IR, UV-Vis, SEM/EDX, ICP-AES, TGA, and DSC techniques. From X-ray technique the molecular formula of the RedHexagonal is $K_{18}\{K[Al_{0.97}Cr_{0.03}(C_2O_4)_3]_6\}Cl.18H_2O$ and the crystal structure is shown in Figure 4.

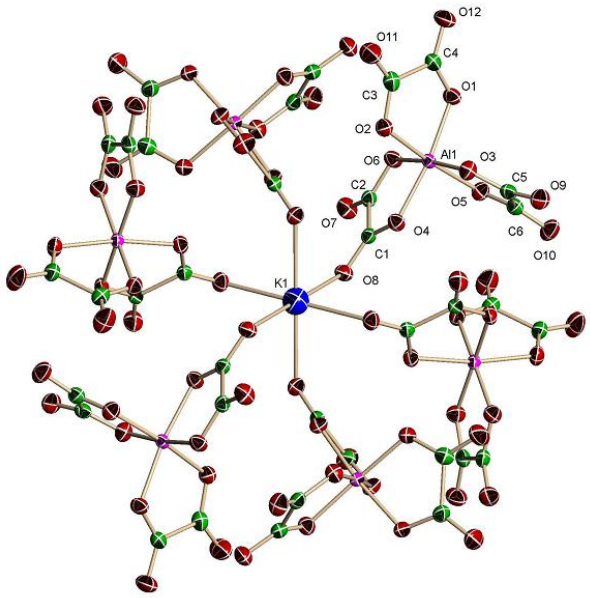

Figure 4 Crystal structure of RedHexagonal (Laongjit, 2004)

This work can be considered as a continuation of Laongjit's work which coverd the syntheses of RedHexagonal, RedCubic, and Blue. Of these three products only the RedHexagonal could be characterized by single crystal X-ray diffractometry (in Laongjit's work). The objective of this part is mainly to further study the remaining products and try to understand the nature of this synthesis reaction as follows.

1. Use other techniques to study some properties of the three products such as ^{13}C-NMR, UV-Vis absorption spectra, etc., to further understand the nature of these products.

2. Characterize the products prepared by the same method but with the amount of $K_3[Cr(C_2O_4)_3]\cdot 3H_2O$ varied to see how the properties of these product change with % Cr doping.